The Journal of Experimental Biology 215, 1218-1230

doi:10.1242/jeb.061176

RESEARCH ARTICLE

CFTR is restricted to a small population of high expresser cells that provide a forskolin-sensitive transepithelial Cl^- conductance in the proximal colon of the possum, *Trichosurus vulpecula*

Shujun Fan*, Natalie Harfoot*, Ray C. Bartolo and A. Grant Butt†

Department of Physiology, School of Medical Sciences, University of Otago, PO Box 913 Dunedin, New Zealand

*These authors contributed equally to this work
†Author for correspondence (grant.butt@stonebow.otago.ac.nz)

SUMMARY

The cystic fibrosis transmembrane conductance regulator (CFTR) is central to anion secretion in both the possum and eutherian small intestine. Here, we investigated its role in the possum proximal colon, which has novel transport properties compared with the eutherian proximal colon. Despite considerable CFTR expression, high doses of the CFTR activator forskolin (EC_{50}≈10 μmol l^{-1}) were required for a modest, CFTR-dependent increase in short-circuit current (I_{sc}) in the proximal colon. Presumably, this is because CFTR is restricted to the apical membrane of a small population of CFTR high expresser (CHE) cells in the surface and upper crypt epithelium. Furthermore, although the forskolin-stimulated I_{sc} was dependent on serosal Na^+, Cl^- and HCO_3^-, consistent with anion secretion, inhibition of the basolateral Na–K–2Cl^- (NKCC1) or Na–HCO_3 (pNBCe1) cotransporters did not prevent it. Therefore, although NKCC1 and pNBCe1 are expressed in the colonic epithelium they do not appear to be expressed in CHE cells. At low doses (IC_{50}≈1 μmol l^{-1}), forskolin also decreased the transepithelial conductance (G_T) of the colon through inhibition of a 4,4′-diisothiocyano-2,2′-stilbenedisulphonic acid-sensitive anion conductance in the basolateral membrane of the CHE cells. This conductance is arranged in series with CFTR in the CHE cells and, therefore, the CHE cells provide a transepithelial Cl^- conductance for passive Cl^- absorption across the epithelium. Inhibition of the basolateral Cl^- conductance of the CHE cells by forskolin will inhibit Na^+ absorption by restricting the movement of its counter-ion Cl^-, assisting in the conversion of the tissue from an absorptive to a secretory state.

Key words: brushtail possum, proximal colon, CFTR, CHE cells, secretion.

INTRODUCTION

The mammalian colon consists of two functionally distinct regions, the proximal and distal colon. The proximal colon is primarily involved in the generation of short chain fatty acids through fermentation of indigestible protein and carbohydrates, while the distal colon functions to regulate the fluid and electrolyte content of the faeces (Karasov and Hume, 1997). For hindgut fermentors, a significant portion of their energy needs is obtained through fermentation in the proximal colon and caecum. This process of fermentation is critically dependent upon the luminal composition, which is determined by fluid and electrolyte transport by the colonic epithelium.

Epithelial ion transport in the proximal colon of the common Australian brushtail possum, *Trichosurus vulpecula*, a marsupial hindgut fermentor, differs from that seen in the proximal colon of eutherian hindgut fermentors, such as the rabbit, guinea pig and rat. In these eutherian mammals, Na^+ absorption by the proximal colon is electroneutral and dependent upon the Na^+/H^+ exchangers NHE3 (Schultheis et al., 1998) and, to a lesser extent, NHE2 (Bachmann et al., 2004), located in the apical membrane of the epithelial cells. Furthermore, secretagogues stimulate electrogenic anion secretion in the eutherian proximal colon and, like all regions of the eutherian intestine, this predominantly involves electrogenic Cl^- secretion, although significant electrogenic HCO_3^- secretion also occurs (Field, 2003). The secretagogue-stimulated Cl^- secretion involves the accumulation of intracellular Cl^- by a basolateral Na–K–2Cl^- cotransporter, NKCC1, and the exit of Cl^- across the apical membrane *via* the cystic fibrosis transmembrane conductance regulator (CFTR) (Kunzelmann and Mall, 2002). HCO_3^- secretion is dependent upon either HCO_3^- transport across the basolateral membrane by a Na–HCO_3 cotransporter (pNBCe1) (Bachmann et al., 2010) or generation of HCO_3^- through hydration of CO_2 (Cuthbert et al., 1999) and exit of HCO_3^- across the apical membrane *via* an anion channel, again most probably CFTR (Grubb, 1997). In contrast, the possum proximal colon exhibits large amounts of amiloride-sensitive electrogenic Na^+ transport (Butt et al., 2002a), which in eutherian mammals is restricted to the distal colon (Kunzelmann and Mall, 2002). However, of particular interest is the observation that membrane-permeable analogues of cAMP and cGMP do not stimulate electrogenic anion secretion in either the proximal or distal colon of the possum (Butt et al., 2002a). Thus, in addition to the marked differences in the absorption of fluid and electrolytes in the possum colon compared with the eutherian colon, there are also significant differences in the secretion of fluid and electrolytes.

In the possum small intestine, cAMP-stimulated electrogenic anion secretion only occurs in the ileum, mainly as a result of the low levels of expression of CFTR in the duodenum and jejunum (Gill et al., 2011). In addition, the ileal response to cAMP-dependent secretagogues involves electrogenic HCO_3^- secretion (Bartolo et al., 2009b), not Cl^- secretion (Bartolo et al., 2009a). This results from the pattern of expression of transporters in the basolateral membrane of the ileal secretory cells. Unlike in the eutherian intestine, NKCC1 is not expressed in the basolateral membrane of the ileal secretory cells of the possum, thus limiting the occurrence of classical bumetanide-sensitive electrogenic Cl^- secretion in response to

secretagogues (Bartolo et al., 2009a). In contrast, pNBCe1 is expressed at high levels in the basolateral membrane of the ileal secretory cells and drives electrogenic HCO_3^- secretion (Bartolo et al., 2009b; Gill et al., 2011).

Unlike in the possum small intestine, there is evidence that the transport proteins associated with electrogenic Cl^- secretion are expressed in the possum colon. High levels of NKCC1 expression have been reported in the proximal colon of the possum (Bartolo et al., 2009a) and CFTR transcript is expressed in possum colon (Demmers et al., 2010). Therefore, the limited secretory response of the possum colon cannot be accounted for by the simple presence or absence of essential transport proteins, as is the case in the possum duodenum and jejunum (Gill et al., 2011). Therefore, in this study we investigated the functional role of CFTR in the possum proximal colon in more detail. Specifically, we determined whether CFTR is expressed in the proximal colon and how its expression in the colonic epithelium compares with that of NKCC1 and pNBCe1, the main basolateral transport proteins associated with electrogenic anion secretion in the intestinal tract of most mammals. In parallel, we used the Ussing short-circuit technique to determine the role of CFTR in the epithelial transport of ions in the possum proximal colon.

MATERIALS AND METHODS

Animals and tissue collection and preparation

Adult Australian common brushtail possums, *Trichosurus vulpecula* (Kerr 1792), were used in this study. They had a live mass greater than 2 kg, and had been trapped and housed as previously described (Butt et al., 2002a). All experimental procedures were performed with the approval of the AgResearch Invermay and Otago University Animal Ethics Committees according to the Animal Welfare Act, 1999. All tissues used in the current study were collected and prepared as previously described (Butt et al., 2002a).

Measurement of epithelial transport

Electrogenic ion transport by the proximal colon was quantified by measuring the short-circuit current (I_{sc}) of the tissues. I_{sc} and transepithelial conductance (G_T) were determined as previously described (Butt et al., 2002a; Butt et al., 2002b). Briefly, after removal of the entire hindgut from the animal, the proximal colon was separated from the rest of the hindgut and the luminal contents flushed with ice-cold Ringer solution (solution 1, Table 1). The tissue was then opened along the mesenteric border, the underlying muscle and connective tissues removed by blunt dissection and the resulting epithelial sheet mounted between two halves of a modified Ussing chamber and superfused with Ringer solution. Oxygenation and stirring of the solutions were achieved *via* gas lift with 95% O_2 and 5% CO_2 when employing bicarbonate-buffered Ringer solution, and with 100% O_2 when employing bicarbonate-free Hepes-buffered Ringer solution. The tissue and solutions were maintained at 37°C by surrounding water jackets. On average, an interval of 30–60 min elapsed between killing the animal and mounting the tissue in the chamber. Throughout the experiment the tissues were constantly short circuited by clamping the transepithelial potential at 0 mV, except for 1 s intervals every 1 or 5 min when the tissue was clamped at ±3 mV and G_T determined.

The Ringer solutions employed in the Ussing chamber experiments are summarized in Table 1. GlyH101 {*N*-(2-naphthalenyl)-[(3,5-dibromo-2,4-dihydroxyphenyl)methylene]glycine hydrazide} was purchased from Merck Ltd (Auckland, New Zealand) and all other reagents were purchased from Sigma-Aldrich Corp. (St Louis, MO, USA). Concentrated stocks of amiloride were prepared in deionized water; forskolin, 5-nitro-2-(3-phenylpropylamino) benzoic acid (NPPB) and GlyH101 in dimethyl sulphoxide (DMSO); bumetanide in ethanol; and 5-(*N*-ethyl-*N*-isopropyl) amiloride (EIPA) in methanol. These drugs were then added as small aliquots of stock solutions to the appropriate side of the tissues. Control experiments demonstrated that equivalent volumes of vehicle had no effect. Acetazolamide was dissolved in a $NaHCO_3$ solution and this solution was used to prepare a Ringer solution containing 1 mmol l^{-1} acetazolamide. 4,4′-Diisothiocyano-2,2′-stilbenedisulphonic acid (DIDS) was prepared as a 10 mmol l^{-1} stock in Ringer solution and this was used to replace the appropriate volume of Ringer solution in the reservoirs, to give a final concentration of 1 mmol l^{-1}.

Western blot analysis of NKCC1, NBC and CFTR

Crude membrane extracts were obtained as described previously (Bartolo et al., 2009a) and the samples separated by SDS-PAGE in 7.5% polyacrylamide gels and electroblotted onto a PVDF membrane (GE Healthcare Biosciences, Auckland, New Zealand). Membranes were blocked with 5% (w/v) skimmed milk powder in Tris-buffered saline containing 0.1% Nonidet-P40 (TBS-NP40) for 1 h, and then incubated for 2 h with specific antibodies: CFTR mouse anti-human (clone M3A7) (1:100 primary; Lab Vision, Fremont, CA, USA; 1:3000 rabbit anti-mouse HRP-conjugated secondary); NKCC1 (N-16) goat polyclonal IgG (1:800 primary; Santa Cruz

Table 1. Composition of Ringer solutions employed in electrophysiological experiments

	Solution 1: $NaCl/HCO_3^-$	Solution 2: Cl^- free	Solution 3: HCO_3^- free	Solution 4: Na^+ free	Solution 5: K^+ free
NaCl	110	0	110	0	115
Sodium gluconate	0	110	25	0	0
NMDG	0	0	0	110	0
KCl	5	0	5	5	0
Potassium gluconate	0	5	0	0	0
$MgSO_4$	0.5	0.5	0.5	0.5	0.5
$CaCl_2$	1	0	1	1	1
Calcium gluconate	0	8	0	0	0
$NaHCO_3$	25	25	0	0	25
NMDG bicarbonate	0	0	0	25	0
Hepes/Tris	10	10	10	10	10
Sodium acetate	10	10	10	0	10
Potassium acetate	0	0	0	10	0
Gas	95% O_2:5% CO_2	95% O_2:5% CO_2	100% O_2	95% O_2:5% CO_2	95% O_2:5% CO_2
pH	7.4	7.4	7.4	7.4	7.4

NMDG, *N*-methyl-D-glucamine.

Biotechnology, Inc., Santa Cruz, CA, USA; 1:5000 donkey anti-goat IgG-HRP-conjugated secondary); NBC rabbit anti-rat NBC serum [1:2000 primary; kindly donated by Dr Bernard Schmitt, Department of Physiology, University of Otago (Schmitt et al., 1999); 1:6000 anti-rabbit HRP-conjugated secondary]. Membranes were then washed with TBS-NP40 and incubated with the respective HRP-conjugated secondary antibodies (GE Healthcare Biosciences) for 2 h. The specificity of the antibodies was determined by pre-absorption with the control peptide for 1 h prior to incubating the membranes (NKCC1 and pNBCe1) or measurements in muscle and inclusion of controls where the primary antibody was omitted (CFTR). Antibodies were detected using enhanced chemiluminescence (GE Healthcare Biosciences).

In situ hybridization of CFTR

In situ hybridization was used to determine the cellular localization of CFTR mRNA in the proximal colon and was carried out as described previously (Gill et al., 2011). The probe for CFTR was amplified from possum intestinal cDNA using the primer pairs previously described (Gill et al., 2011). The resulting cDNA was subcloned using the Promega pGem® T Easy vector system (Promega Corporation, Madison, WI, USA) and [^{33}P]dUTP (NZ Scientific Ltd, Auckland, New Zealand) labelled sense and anti-sense probes were transcribed using an *in vitro* transcription kit (Riboprobe® *in vitro* transcription systems, Promega Corporation) according to the manufacturer's instructions. Hybridization and detection of the probe were carried out as described previously (Bartolo et al., 2009a).

Immunolocalization of CFTR, pNBCe1 and NKCC1 proteins

Immunolocalization of CFTR, pNBCe1 and NKCC1 was carried out as described previously (Bartolo et al., 2009a; Bartolo et al., 2009b; Gill et al., 2011). Briefly, proximal colonic tissue samples were embedded in OCT compound (Siemens Medical Solutions, Erlangen, Germany) and snap frozen in isopentane pre-cooled in liquid nitrogen. Sections (10 µm) were placed on slides coated in 2% 3-aminopropyltriethoxysilane (Sigma-Aldrich Corp.), air dried for 10 min and stored at –80°C until required. For immunohistochemistry, sections were rinsed in PBS (in mmol l^{-1}: 137 NaCl, 10 phosphate, 2.7 KCl; pH 7.4) for 5 min, fixed in 0.4% paraformaldehyde for 10 min and blocked in 1% donkey serum in PBS for 30 min. The sections were then incubated with combinations of primary (4 h) and then secondary (2 h) antibodies to determine the co-localization of CFTR with NKCC1 or pNBCe1, and the co-localization of NKCC1 with pNBCe1 in the epithelial layer of the proximal colon, followed by incubation with DAPI (Sigma-Aldrich Corp.; 100 ng ml^{-1} in PBS) for 20 min. Primary antibody dilutions were as follows: mouse anti-human CFTR, 2 µg ml^{-1} in PBS; goat anti-human NKCC1, 1 µg ml^{-1} in PBS; and rabbit anti-rat NBC, diluted 1:300 in PBS; incubation was carried out for 4 h. The sections were then washed in PBS and incubated with the respective secondary antibodies at the following dilutions: Texas Red donkey anti-mouse IgG, diluted 1.5 µg ml^{-1} in PBS (Jackson ImmunoResearch Laboratories, Inc., West Grove, PA, USA); and FITC-conjugated donkey anti-rabbit IgG, diluted 1.5 µg ml^{-1} in PBS (Jackson ImmunoResearch Laboratories, Inc.). Two secondary antibodies were required for the detection of NKCC1: Alexa Fluor® 546 donkey anti-goat (when co-localized with pNBCe1; 2 µg ml^{-1} in PBS; Invitrogen Ltd, Auckland, New Zealand) and FITC-conjugated rabbit anti-goat IgG (when co-localized with CFTR; 1.5 µg ml^{-1} in PBS, Invitrogen). Finally, the sections were washed in PBS, mounted in Vectashield® mounting medium (Vector Laboratories, Burlingame, CA, USA) and examined and photographed using a confocal scanning laser system (Zeiss 510 LSM; Carl Zeiss GmbH, Jena, Germany).

Statistics

The results of electrophysiological experiments are presented as either individual recordings or means ± s.e.m., *N*=number of animals. Differences between means were tested, where appropriate, with either Student's unpaired two-tailed *t*-test or one-way ANOVA with Dunnett's *post hoc* test as indicated in the figure legends. Differences were considered to be statistically significant where $P<0.05$.

RESULTS

Expression of NKCC1, pNBCe1 and CFTR in the colon

Typically, in the intestinal tract CFTR functions as an apical anion channel associated with Cl^- or HCO_3^- secretion. Therefore, we initially considered the expression and distribution of CFTR relative to that of NKCC1 and pNBCe1 within the colonic epithelium. There were relatively high levels of expression of CFTR in the proximal colon, with lower levels in the distal colon. In contrast, the expression of pNBCe1 was comparable in the two regions of the colon and, as seen previously (Bartolo et al., 2009a), NKCC1 was expressed at high levels in the proximal colon and similar levels were seen in the distal colon (Fig. 1). Because we are primarily interested in the novel transport characteristics of the proximal colon, all subsequent measurements focused on the role of CFTR in the proximal colon.

The overall structure of the possum proximal colon is comparable to that of the eutherian mammals with a flat surface epithelium and an extensive elaboration of the epithelial surface area by a large number of invaginations forming crypts. Within this structure, immunoreactivity for both NKCC1 and pNBCe1 was localized to the basolateral membrane of the epithelial cells (Fig. 2E,F) but immunoreactivity associated with NKCC1 was present in the lower half of the crypts, whereas that associated with pNBCe1 was present in cells in the upper half of the crypts and the surface epithelium (Fig. 2A). In contrast, immunoreactivity for CFTR was restricted to

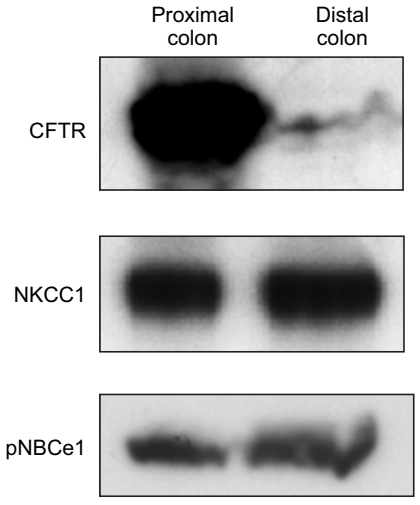

Fig. 1. Western blots showing that the cystic fibrosis transmembrane conductance regulator (CFTR), the Na–K–2Cl^- cotransporter (NKCC1) and the pancreatic variant of the electrogenic Na–HCO_3 cotransporter (pNBCe1) are expressed in the possum colon.

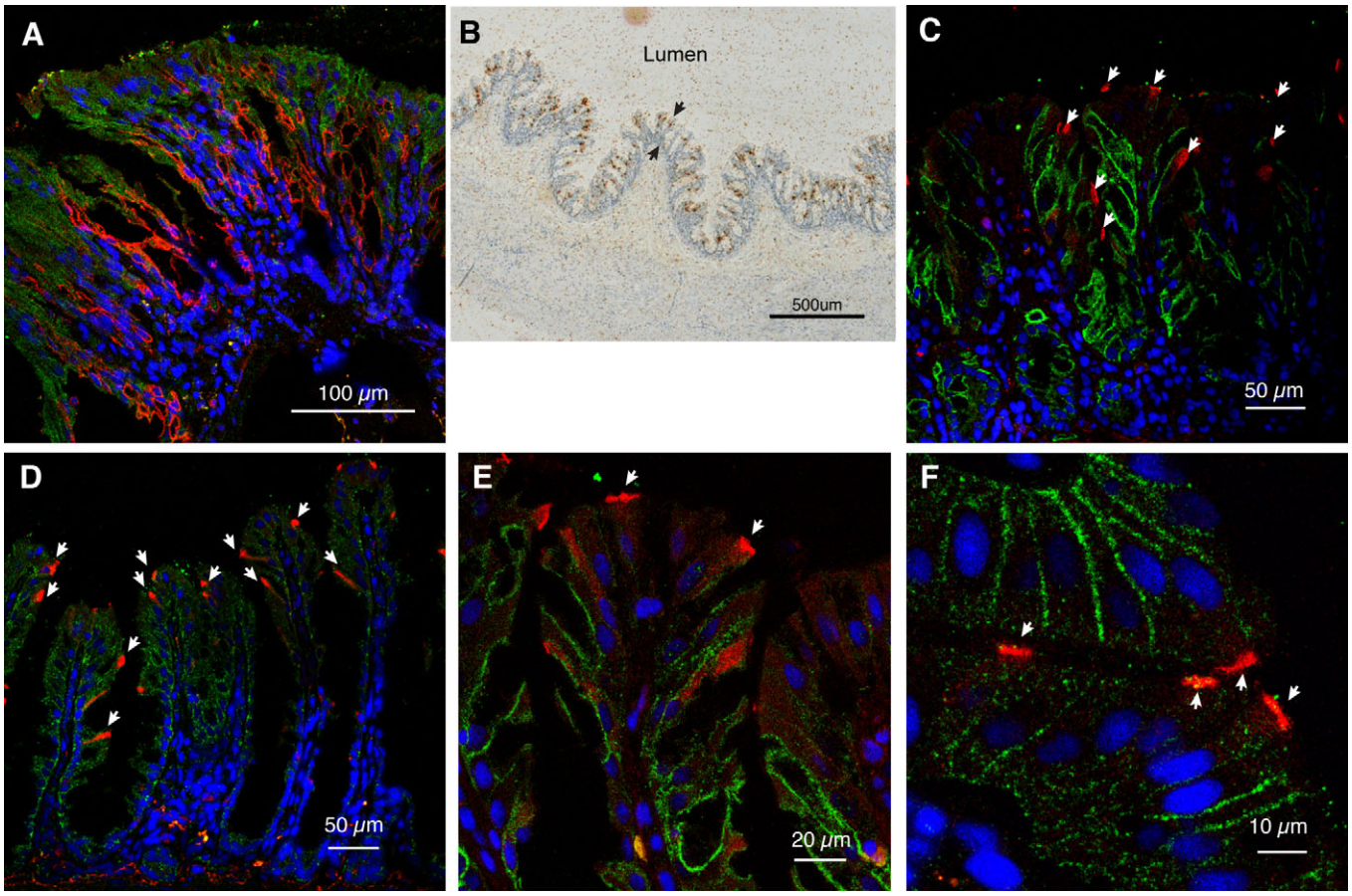

Fig. 2. Localization of NKCC1, pNBCe1 and CFTR in the proximal colonic epithelium of the possum using *in situ* hybridization and immunohistochemistry. (A) Transverse section showing NKCC1 immunoreactivity (red) is located mainly in the lower half of the crypts whereas pNBCe1 immunoreactivity (green) is concentrated in the upper half of the crypts and the surface epithelium. (B) CFTR mRNA, indicated by brown dots, was distributed in a punctate fashion in the upper half of the crypts and surface epithelium. Arrows delineate the epithelia layer with surface cells facing the lumen. (C) The immunoreactivity for CFTR (red and indicated by arrows) had a similar punctate distribution to that of the mRNA and was located in cells in the upper regions of the crypts and surface epithelium, separate from NKCC1 (green) in the lower half of the crypts. (D) In contrast, the distribution of CFTR immunoreactivity (red and indicated by arrows) overlapped that of pNBCe1 (green), both being located in the upper half of the crypts and surface cells. In those cells containing CFTR immunoreactivity (red), it was localized in the apical pole and concentrated in the region of the apical membrane (E,F). (E) CFTR (red and indicated by arrows) immunoreactivity does not appear to be present in the same cells in which NKCC1 immunoreactivity (green) was evident. (F) Because of the close association of the basolateral membranes of the CFTR high expresser (CHE) cells (indicated by arrows) and surrounding epithelial cells, which exhibit high levels of pNBCe1 immunoreactivity (green), it is not possible to determine the levels of expression of pNBCe1 in the CHE cells. In A and C–F the nuclei are stained blue.

a small number of cells located in the surface epithelium and the upper third of the crypts (Fig. 2C,D). A similar pattern of distribution was evident from measurements of the location of CFTR transcript by *in situ* hybridization (Fig. 2B). In those cells exhibiting CFTR immunoreactivity, high levels of expression were demonstrated and most of the immunoreactivity was concentrated at the apical pole of the cell, with lower levels of CFTR immunoreactivity in the cytoplasm and extending from the apical membrane towards the nuclei (Fig. 2E,F). The immunoreactivity associated with CFTR and NKCC1 was located in different regions of the crypt–surface cell axis and the two transporters do not appear to be present in the same cells in the proximal colon (Fig. 2E). In contrast, immunoreactivity associated with CFTR and pNBCe1 was present in the same region of the crypt–surface cell axis. Consequently, because of the close association of the surrounding cell membranes, which contain pNBCe1 immunoreactivity, it was not possible to exclude the expression of pNBCe1 in the CFTR high expresser (CHE) cell basolateral membrane (Fig. 2F).

The effect of forskolin on the I_{sc} and G_T of the proximal colon

To gain some insight into the function of CFTR in the proximal colon, we investigated the effect of stimulation of CFTR on the electrical properties of the proximal colonic epithelium mounted in Ussing chambers. The tissues were bathed in NaCl/HCO_3 Ringer solution (solution 1, Table 1) and, to maximize the chances of observing a response associated with activation of CFTR, they were constantly short-circuited and pre-treated with a high dose of mucosal amiloride (100 μmol l^{-1}) to inhibit electrogenic Na^+ absorption, before stimulation with forskolin. Forskolin was chosen because it directly stimulates adenylate cyclase to increase intracellular cAMP (Seamon et al., 1981) and has been shown to stimulate cloned possum CFTR (Demmers et al., 2010).

As previously observed (Butt et al., 2002a), the proximal colon had a large spontaneous I_{sc} (I_{sc} initial=183±14 μA cm^{-2}, N=20), and the majority of this I_{sc} was inhibited by mucosal amiloride (I_{sc} after amiloride=18±3 μA cm^{-2}, P<0.0001) (Fig. 3A). Interestingly, the proximal colon had a relatively high G_T before amiloride

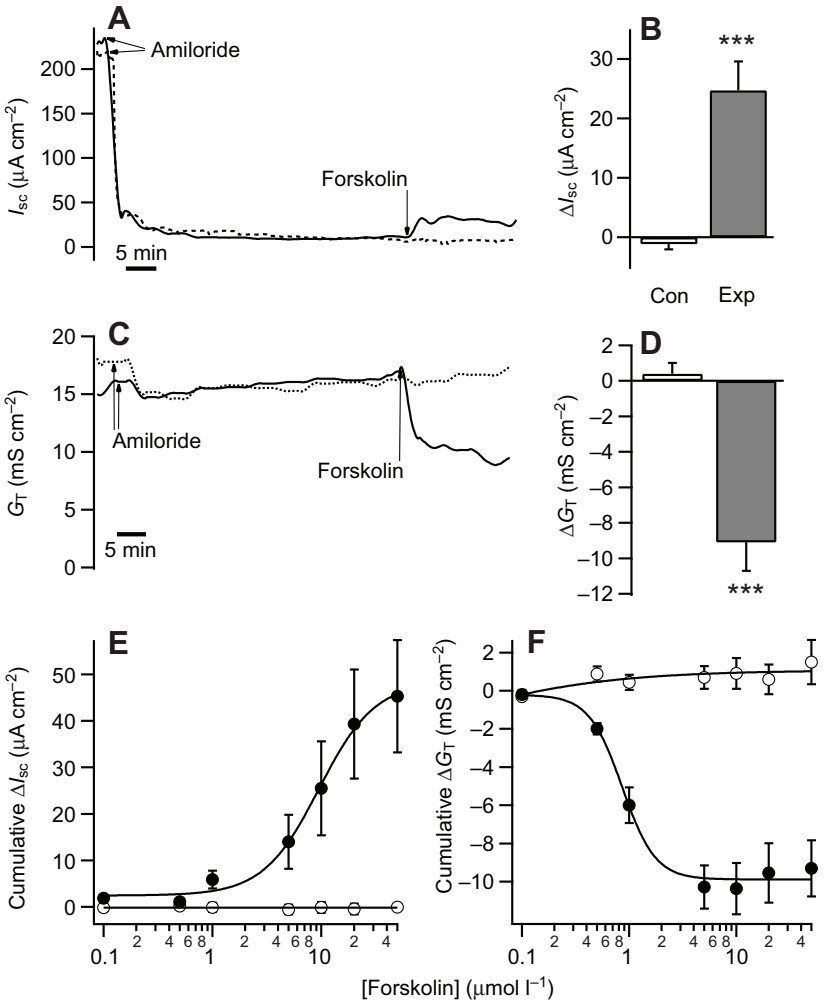

Fig. 3. The effect of forskolin following pre-treatment with mucosal amiloride (100 μmol l^{-1}) on electrogenic ion transport by the possum proximal colon. (A,C) Representative experiment showing variations in short-circuit current (I_{sc}) and transepithelial conductance (G_T) stimulated by forskolin (20 μmol l^{-1} mucosal and serosal). (B,D) The change in I_{sc} (ΔI_{sc}) and G_T (ΔG_T) stimulated by forskolin (Exp) compared with changes in control tissues (Con) treated with vehicle. N=20. Asterisks indicate significant difference (***P<0.001) from control, Student's unpaired t-test. (E,F) Cumulative ΔI_{sc} and ΔG_T in tissues treated with increasing doses of mucosal and serosal forskolin. Open symbols, control tissues treated with vehicle; filled symbols, experimental tissues treated with forskolin. N=7. ΔI_{sc} and ΔG_T in response to forskolin fitted with Hill equation. $\Delta I_{sc,max}$=48±3 μA cm^{-2}, EC_{50}=9.5±1.26 μmol l^{-1} and $\Delta G_{T,max}$=–9.9±0.2 mS cm^{-2}, IC_{50}=0.86±0.24 μmol l^{-1}.

(27±2.3 mS cm^{-2}) and there was only a small decrease in G_T associated with the inhibition of I_{sc} by amiloride (G_T after amiloride=23±2.0 mS cm^{-2}, P<0.0001, N=20) (Fig. 3C). Unlike previous studies that utilized membrane-permeable analogues of cAMP (Butt et al., 2002a), high doses of forskolin (20 μmol l^{-1} mucosal and serosal) stimulated a modest, but significant (P<0.001, N=20) increase in I_{sc} from 18±3 to 43±4 μA cm^{-2} (Fig. 3A,B). Associated with this forskolin-stimulated I_{sc} (ΔI_{sc}) was a significant (P<0.001) decrease in G_T (ΔG_T), from 20.2±1.5 to 12.8±1 mS cm^{-2} (Fig. 3C,D, N=20). Both the stimulation of I_{sc} and inhibition of G_T by forskolin were dose dependent, although with markedly different characteristics. The stimulation of I_{sc} by forskolin required relatively high doses, with an EC_{50}=9.5 μmol l^{-1} forskolin (Fig. 3E), whereas the inhibition of G_T occurred at lower doses with an IC_{50} of 1 μmol l^{-1} (Fig. 3F). The forskolin-stimulated ΔI_{sc} seen in the presence of amiloride is consistent with the stimulation of anion secretion and it is evident that an inflection in the dose–response curve for G_T occurs at ~10 μmol l^{-1} forskolin, where further additions of forskolin result in a small increase in G_T. This is consistent with an increase in G_T associated with secretion. A comparison of the ΔG_T induced by 5 μmol l^{-1} forskolin and the subsequent ΔG_T associated with the addition of 20 μmol l^{-1} forskolin indicates that the conductance pathway inhibited by forskolin amounts to 10.4±1.5 mS cm^{-2}, whereas the conductance pathway associated with the stimulation of I_{sc} is 1.1±0.2 mS cm^{-2}. Both the initial decrease in G_T and the subsequent increase in G_T are significantly (P<0.05) different to the time-dependent changes in G_T of the control tissues. This, combined with the marked difference in the EC_{50} values for the effect of forskolin on I_{sc} and G_T, indicates that forskolin stimulates two distinct processes in the possum proximal colon.

The forskolin-induced changes in I_{sc} and G_T are dependent upon CFTR

NPPB and GlyH101 are effective inhibitors of possum (p)CFTR (Gill et al., 2011). Therefore, to determine whether the forskolin-induced changes in I_{sc} and G_T are dependent upon pCFTR, we considered the effects of NPPB and GlyH101 on the response to forskolin. Because GlyH101 is known to also inhibit Ca^{2+}-activated Cl^- channels at higher doses, the effect of DIDS, which blocks Ca^{2+}-activated Cl^- channels (Yang et al., 2008), but not possum CFTR (Gill et al., 2011), was also investigated. Four tissues from each animal were pre-treated with amiloride and then two of the tissues were stimulated with forskolin (20 μmol l^{-1} mucosal and serosal) and, when the I_{sc} response to forskolin had reached a steady state, mucosal NPPB (100 μmol l^{-1}), GlyH101 (50 μmol l^{-1}) or DIDS (1 mmol l^{-1}) was added to one of the stimulated and unstimulated tissues. The other two tissues served as time-matched controls.

Following pre-treatment with amiloride, the spontaneous I_{sc} in the unstimulated tissues was <20 μA cm^{-2} and mucosal NPPB, GlyH101 and DIDS had no effect upon this I_{sc} (data not shown).

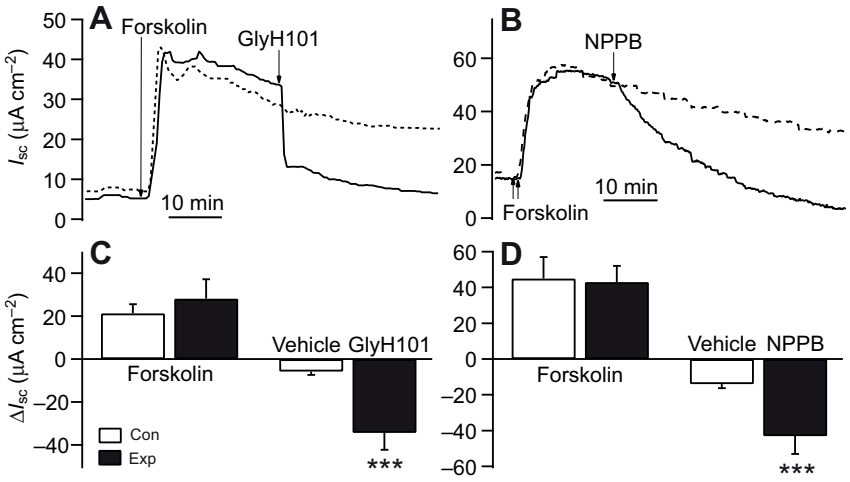

Fig. 4. The effect of mucosal *N*-(2-naphthalenyl)-[(3,5-dibromo-2,4-dihydroxyphenyl)methylene]glycine hydrazide (GlyH101) and 5-nitro-2-(3-phenylpropylamino) benzoic acid (NPPB) on the forskolin-stimulated I_{sc} in the proximal colon. Paired tissues were stimulated with forskolin (20 μmol l^{-1} mucosal and serosal) and once the response had reached a steady state either GlyH101 (50 μmol l^{-1}) or NPPB (100 μmol l^{-1}) was added to the experimental tissue (solid line), while an equivalent volume of the vehicle (DMSO) was added to the control tissue (broken line). (A,B) Representative experiments showing the effect of (A) mucosal GlyH101 and (B) mucosal NPPB on the I_{sc}. (C,D) A summary of the effects of (C) GlyH101 and (D) NPPB on the forskolin-stimulated I_{sc}. *N*=6 for C, *N*=7 for D. Asterisks indicate significant difference (***P<0.001) from control tissues, Student's unpaired *t*-test.

In contrast, following stimulation with forskolin (20 μmol l^{-1}), both mucosal GlyH101 (Fig. 4A,B) and NPPB (Fig. 4C,D) markedly reduced the I_{sc}, effectively inhibiting the forskolin-stimulated ΔI_{sc}, whereas after 30 min DIDS had not significantly reduced the forskolin-stimulated I_{sc} (ΔI_{sc} DIDS=–16±μA cm^{-2}) when compared with the spontaneous decline in I_{sc} (ΔI_{sc} control=–13±2.1 μA cm^{-2}, *N*=5) in the time-matched control tissues. These data indicate that forskolin stimulates a CFTR-dependent increase in I_{sc} in the proximal colon, and the increase in I_{sc} induced by forskolin does not appear to involve an appreciable Ca^{2+}-activated Cl^- conductance in the possum proximal colon – a conclusion supported by the observation that neither carbachol (100 μmol l^{-1}, serosal) nor thapsigargin (1 μmol l^{-1}, mucosal and serosal) had an effect on the I_{sc} or G_T in the proximal colon (data not shown).

Significantly, while mucosal GlyH101 and NPPB had little effect on the spontaneous I_{sc}, they both markedly decreased the spontaneous G_T of the tissues (Fig. 5A–C). However, following stimulation with forskolin, which decreases G_T, neither mucosal GlyH101 (Fig. 5D,E) nor NPPB (Fig. 5F) had a further effect on G_T. Mucosal DIDS had no effect on the spontaneous G_T (following 30 min treatment with 1 mmol l^{-1} DIDS, ΔG_T=–0.4±0.6 mS cm^{-2}, *N*=5) or G_T following stimulation with forskolin (following 30 min treatment with 1 mmol l^{-1} DIDS, ΔG_T=–0.7±0.4 mS cm^{-2}, *N*=5).

The forskolin-stimulated I_{sc} is independent of NKCC1 and pNBCe1

To determine whether NKCC1 and pNBCe1 were involved in the I_{sc} response to forskolin we considered the effects of bumetanide and DIDS, inhibitors of NKCC1 and pNBCe1, respectively, on the I_{sc} response to forskolin. In the initial experiment paired tissues were pre-treated with mucosal amiloride (100 μmol l^{-1}) plus serosal bumetanide (100 μmol l^{-1}) then, after ~30 min, both tissues were

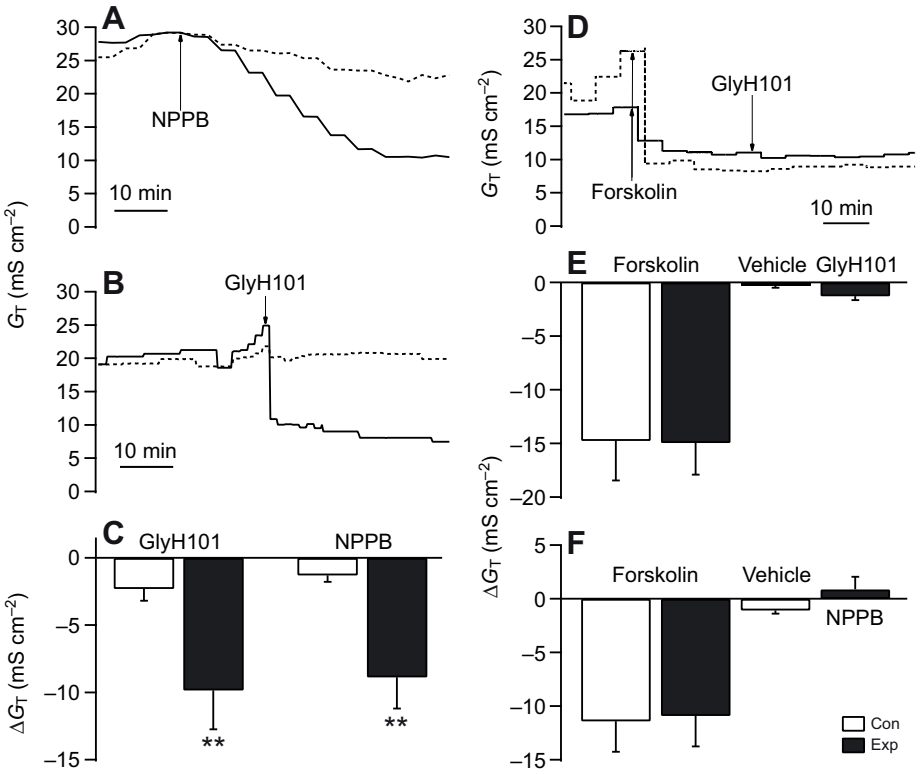

Fig. 5. The effect of mucosal GlyH101 and NPPB on the transepithelial conductance (G_T) of the proximal colon. Representative examples of the effect of (A) mucosal NPPB (100 μmol l^{-1}) and (B) mucosal GlyH101 (50 μmol l^{-1}) on the spontaneous G_T of the proximal colon. (C) A comparison of the change in G_T (ΔG_T) induced by either GlyH101 (50 μmol l^{-1}, *N*=6) or NPPB (100 μmol l^{-1}, *N*=8) in the experimental tissues (Exp), compared with the ΔG_T induced by the vehicle alone in paired control tissues (Con). (D) Representative experiment showing the effect of GlyH101 (40 μmol l^{-1}) on the G_T following stimulation with forskolin (20 μmol l^{-1}). Tissues were stimulated with forskolin and then GlyH101 was added to the experimental tissue (solid line) while an equivalent volume of the vehicle (DMSO) was added to the control tissue (broken line). (E) The ΔG_T induced by forskolin and the subsequent addition of DMSO (Con) or GlyH101 (Exp). *N*=6. (F) Results from a similar set of experiments were NPPB was added following stimulation with forskolin, rather than GlyH101. *N*=7. Asterisks indicate significant difference (**P<0.01) from control tissues, Student's unpaired *t*-test.

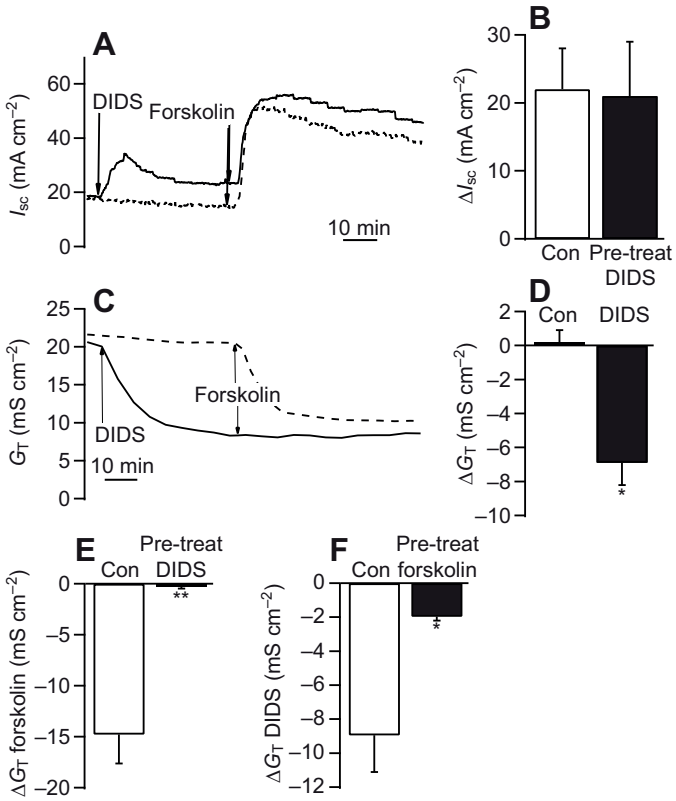

Fig. 6. Effect of serosal 4,4′-diisothiocyano-2,2′-stilbenedisulphonic acid (DIDS) on I_{sc} and G_T of the proximal colon. (A) Representative experiment showing the effect of treatment with serosal DIDS (1 mmol l^{-1}) on the spontaneous I_{sc} and the subsequent response to forskolin (20 μmol l^{-1} mucosal and serosal). (B) Mean change in I_{sc} (ΔI_{sc}) stimulated by forskolin in control (Con) tissues and tissues pre-treated with DIDS. (C) Variation in G_T of tissues shown in A. (D) Change in spontaneous G_T (ΔG_T) induced by serosal DIDS compared with ΔG_T of control tissues (Con) treated with vehicle. (E) Forskolin-induced ΔG_T in control tissues (Con) and tissues pre-treated with serosal DIDS. (F) DIDS-induced ΔG_T in control tissues (Con) and tissues stimulated with forskolin. B and D–F, N=6. Asterisks indicate significant difference (*P<0.05, **P<0.01) from control values, Student's unpaired t-test.

stimulated with forskolin (20 μmol l^{-1} mucosal and serosal). Treatment with bumetanide did not inhibit the response to forskolin, but actually increased it (ΔI_{sc} control=21±2.8 μA cm^{-2}; ΔI_{sc} bumetanide=34±2.3 μA cm^{-2}, N=30, P<0.01). This was due to the stimulation of a small, but significant amount of K^+ secretion by forskolin (S.F. and A.G.B., unpublished results). A similar protocol was employed to assess the effects of inhibition of pNBCe1 on the forskolin response, except the two tissues were pre-treated with mucosal amiloride and serosal bumetanide (100 μmol l^{-1}) to eliminate changes in I_{sc} associated with both Na^+ absorption and K^+ secretion. DIDS (1 mmol l^{-1} serosal) was then added to one of the paired tissues and ~30 min later the two tissues were stimulated with forskolin. Serosal DIDS resulted in a small increase in spontaneous I_{sc} (ΔI_{sc} DIDS=12±3 μA cm^{-2}, N=6), but it had little effect on the subsequent stimulation of I_{sc} by forskolin (Fig. 6A,B). Although serosal DIDS did not inhibit the forskolin-induced ΔI_{sc}, it had a marked effect on the spontaneous G_T of the tissues, resulting in a progressive decrease in G_T from 17.3±1.5 to 11.3±1.6 mS cm^{-2} (P<0.05, N=6, Fig. 6C). Serosal DIDS stimulated a rapid increase in spontaneous I_{sc}, but the DIDS-induced decrease in G_T was much slower (Fig. 6). This suggests that the two were unrelated, a conclusion supported by the observation that DIDS stimulated a similar increase in I_{sc} (ΔI_{sc} DIDS=8±4 μA cm^{-2}) after stimulation with forskolin, but without a change in G_T (Fig. 6C,F). Furthermore, if tissues were stimulated with serosal DIDS and, once the I_{sc} response had reached a steady state (ΔI_{sc} DIDS=11±2.4 μA cm^{-2}, N=6), mucosal GlyH101 was added, GlyH101 did not inhibit the DIDS-stimulated I_{sc} (ΔI_{sc} GlyH101 after DIDS=–2.8±3.4 μA cm^{-2}, whereas in the absence of DIDS ΔI_{sc} GlyH101=–3.7±1.2 μA cm^{-2}), indicating that the DIDS-stimulated I_{sc} does not involve CFTR. Notably, not only did pre-treatment with forskolin reduce the effect of DIDS on G_T but also pre-treatment with DIDS reduced the forskolin-induced decrease in G_T (Fig. 6C,E). This suggests that DIDS and forskolin are acting on a common transepithelial conductance.

In a number of intestinal epithelia, HCO_3^- secretion results from the hydration of CO_2 by carbonic anhydrase (Knutson et al., 1995; Leppilampi et al., 2005). To determine whether this was operating in the possum proximal colon, paired tissues were pre-treated with mucosal amiloride and serosal bumetanide and then one was incubated with acetazolamide (1 mmol l^{-1}, mucosal and serosal) for ~30 min before stimulation of both tissues with forskolin. This had no effect on the forskolin-stimulated ΔI_{sc} (ΔI_{sc} forskolin control=29±13 μA cm^{-2} and following incubation with acetazolamide ΔI_{sc} forskolin=23±7 μA cm^{-2}, N=4). Similarly, pre-treatment with acetazolamide and serosal DIDS (1 mmol l^{-1}), to prevent compensatory up regulation of alternative transporters (Gawenis et al., 2010), had no effect on the forskolin-stimulated I_{sc} and nor did the NHE inhibitor EIPA (100 μmol l^{-1} serosal, data not shown), demonstrating that the secretion of HCO_3^- produced by hydration of CO_2 does not contribute to the forskolin-stimulated ΔI_{sc}.

The ion dependence of the forskolin-induced changes in I_{sc} and G_T

To gain further insight into the basis of the forskolin-induced changes in I_{sc} and G_T, the ionic dependence of the response to forskolin was investigated. Initially, to determine whether there was any Na^+ dependence of the forskolin-stimulated ΔI_{sc}, the response of tissues in which all of the Na^+, in either the mucosal or serosal solutions, had been replaced with the impermeant cation N-methyl D-glucamine (NMDG) (solution 4, Table 1) was compared with paired control tissues. Similarly, the possible stimulation of electrogenic K^+ absorption by forskolin was excluded by replacing the mucosal K^+ with Na^+ (solution 5, Table 1). The replacement of mucosal K^+ with Na^+ or mucosal Na^+ with NMDG had no effect on the subsequent response to forskolin (data not shown). However, the replacement of serosal Na^+ with NMDG completely inhibited the response to forskolin (in serosal Na^+ Ringer solution ΔI_{sc} forskolin=30±4.1 μA cm^{-2} and in serosal Na^+-free Ringer solution ΔI_{sc} forskolin=0.7±3.4 μA cm^{-2}, N=4, P<0.01), indicating that a serosal Na^+-dependent process is involved in the I_{sc} response to forskolin.

To establish the anion dependence of the forskolin response, paired tissues were bathed in either NaCl/HCO_3 Ringer solution (solution 1, Table 1) or HCO_3^--free NaCl/Hepes-buffered Ringer solution (solution 3, Table 1). In a second set of experiments, one tissue was again bathed in NaCl/HCO_3 Ringer solution (solution 1, Table 1) while the other was bathed in Cl^--free sodium gluconate/HCO_3^- Ringer solution (solution 2, Table 1). In all cases, the tissues were pre-treated with mucosal amiloride (100 μmol l^{-1}) and serosal bumetanide (100 μmol l^{-1}) before stimulation with forskolin (20 μmol l^{-1}, mucosal and serosal). In the absence of either HCO_3^- or Cl^- the forskolin-stimulated ΔI_{sc} was eliminated (Fig. 7A), indicating that the forskolin response was dependent on both anions.

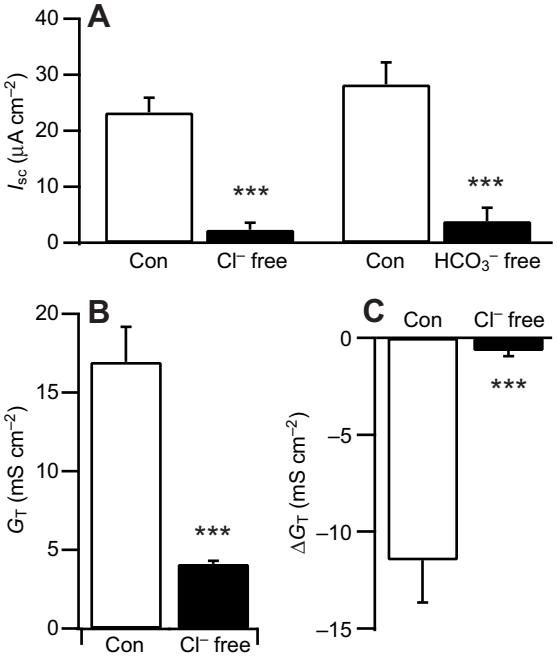

Fig. 7. The effect of Cl^--free or HCO_3^--free Ringer solution on the response of the proximal colon to forskolin. (A) Mean increase in I_{sc} (ΔI_{sc}) stimulated by forskolin (20 μmol l^{-1} mucosal and serosal) in Cl^--free (solution 2, Table 1) or HCO_3^--free (solution 3, Table 1) Ringer solution compared with the response of control tissues bathed in NaCl/HCO_3^- Ringer solution (Con). (B) G_T of tissues bathed in NaCl/HCO_3^- Ringer solution (Con) compared with tissues bathed in Cl^--free Ringer solution. (C) Change in G_T (ΔG_T) induced by forskolin in Cl^--free Ringer solution compared with the change induced in control tissues bathed in NaCl/HCO_3^- Ringer solution. N=16. Asterisks indicate significant difference (***P<0.001) from respective control, Student's unpaired t-test.

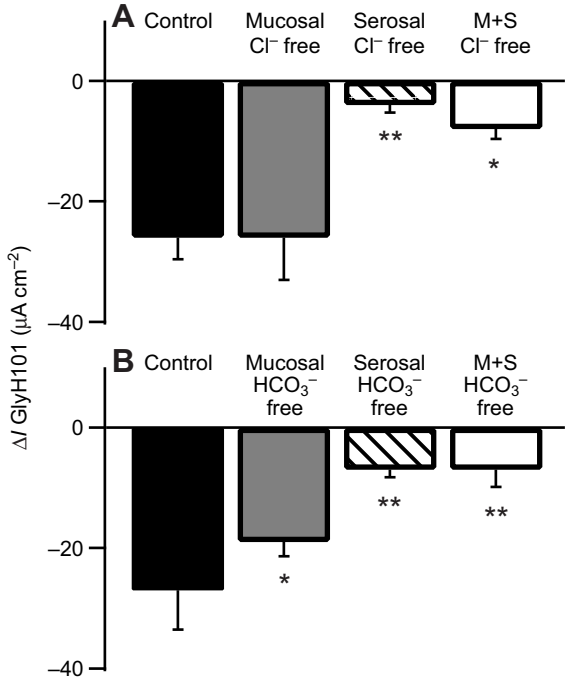

Fig. 8. The effect of replacement of (A) Cl^- or (B) HCO_3^- in the mucosal, serosal or mucosal and serosal (M+S) solutions on the GlyH101-sensitive current (ΔI GlyH101) following stimulation with forskolin. The tissues were bathed in the Ringer solution as indicated, stimulated with forskolin (20 μmol l^{-1} mucosal and serosal) and then, in the continued presence of forskolin, GlyH101 (50 μmol l^{-1}) was added to the mucosal side and ΔI GlyH101 calculated from the transepithelial current before and after GlyH101. N=6. Asterisks indicate significant difference (*P<0.05, **P<0.01) from control value, ANOVA with Dunnett's *post hoc* test.

To confirm this was associated with anion secretion, the effect of replacement of either mucosal or serosal Cl^- or HCO_3^- on the forskolin response was determined. Four tissues from each animal were used; one tissue served as a control and was bathed with mucosal and serosal NaCl/HCO_3^- Ringer solution (solution 1, Table 1). In the other tissues, either Cl^- (solution 2, Table 1) or HCO_3^- (solution 3, Table 1) was removed from the mucosal, the serosal or the mucosal and serosal side. Because two of the tissues were bathed in asymmetric solutions resulting in current flow not associated with active transport (see below), the magnitude of the mucosal GlyH101-sensitive (50 μmol l^{-1}) current (ΔI GlyH101) following stimulation with forskolin (20 μmol l^{-1}, mucosal and serosal) was used to quantify the effect of the ion substitutions on the response to forskolin. The removal of Cl^- from the mucosal solution had no effect on the magnitude of the ΔI GlyH101, whereas the removal of serosal Cl^- had an effect comparable to that of removal of Cl^- from both the mucosal and serosal solutions (Fig. 8A). Qualitatively similar results were obtained with the asymmetric removal of CO_2/HCO_3^- (Fig. 8B). Serosal CO_2/HCO_3^--free Ringer solution reduced the magnitude of the ΔI GlyH101 to a similar extent to serosal and mucosal CO_2/HCO_3^--free Ringer solution. However, the removal of mucosal CO_2/HCO_3^- also partially inhibited the ΔI GlyH101, although to a smaller extent (Fig. 8B). These data support the proposal that forskolin stimulates a Cl^- and HCO_3^--dependent, electrogenic secretory response.

A cellular transepithelial Cl^- conductance is present in the possum proximal colon

As well as inhibiting the forskolin-stimulated ΔI_{sc}, the replacement of Cl^- with the impermeant anion gluconate also prevented the decrease in G_T induced by forskolin (Fig. 7C). This was associated with a large decrease in the G_T of the tissues bathed in Cl^--free Ringer solution (Fig. 7B) and is consistent with the presence of a transepithelial Cl^- conductance in the proximal colon that is inhibited by forskolin.

This proposal is supported by the observation that a forskolin-sensitive Cl^- current (I_{Cl}) developed in the presence of a transepithelial Cl^- gradient. When the proximal colon was bathed in NaCl/HCO_3^- Ringer solution (solution 1, Table 1) on the mucosal side and Cl^--free Ringer solution (solution 2, Table 1) on the serosal side (ΔCl_{ms}) a large I_{Cl} was measured across the epithelium, which was rapidly and almost completely inhibited by forskolin (20 μmol l^{-1}) (Fig. 9A,B). The inhibitory effect of forskolin was dose dependent and the IC_{50} for this effect of forskolin was comparable to the IC_{50} for the forskolin-induced decrease in G_T of tissues bathed in symmetrical Ringer solution (Fig. 10). The generation of a forskolin-sensitive current by a transepithelial ion gradient was dependent upon Cl^-, as in the presence of an equivalent mucosal to serosal Na^+ gradient (Na^+ replaced with NMDG, solution 4, Table 1) the Na^+ current (I_{Na}) was only 82±10 μA cm^{-2} (N=6) and was unaffected by forskolin (I_{Na} after forskolin=84±10 μA cm^{-2}).

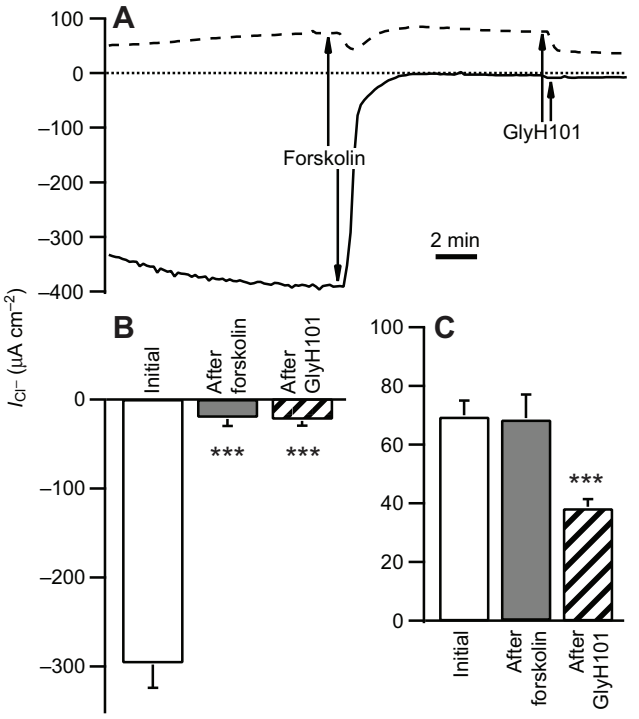

Fig. 9. A Cl^- gradient across the possum colon results in a transepithelial current that is inhibited by forskolin. (A) Representative experiment showing the effect of forskolin (20 μmol l^{-1} mucosal and serosal) followed by GlyH101 (50 μmol l^{-1}, mucosal) on the Cl^- current (I_{Cl}) in tissues bathed in either mucosal NaCl/HCO_3^- Ringer solution (solution 1, Table 1) and serosal sodium gluconate/HCO_3^- Ringer solution (solution 2, Table) (mucosal to serosal Cl^- gradient) or mucosal sodium gluconate/HCO_3^- Ringer solution and serosal NaCl/HCO_3^- Ringer solution (serosal to mucosal Cl^- gradient). (B,C) The I_{Cl} before (Initial) and after forskolin addition, and after GlyH101 (50 μmol l^{-1}) in the continued presence of forskolin in tissues bathed in (B) a mucosal to serosal Cl^- gradient and (C) a serosal to mucosal Cl^- gradient. N=8. Asterisks indicate significant difference (***P<0.001) from control, ANOVA with Dunnett's *post hoc* test.

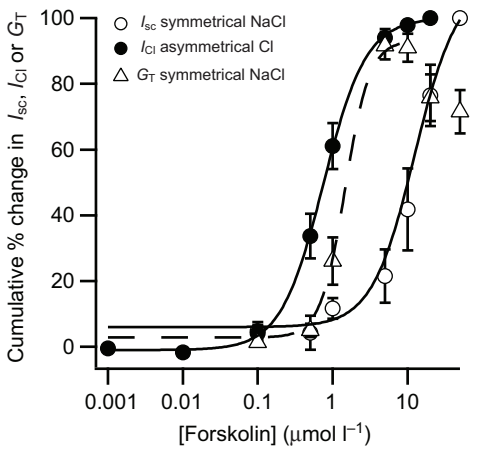

Fig. 10. A comparison of the forskolin dose dependency of the change in I_{sc} or G_T of tissues bathed in symmetrical NaCl/HCO_3^- Ringer solution (solution 1, Table 1) and change in I_{Cl} of tissues bathed in mucosal NaCl/HCO_3^- and serosal sodium gluconate/HCO_3^- Ringer solution (mucosal to serosal Cl^- gradient). All values are expressed as a percentage of the maximal change. N≥5. Curves fitted with Hill equation. Data for symmetrical Ringer solution are from Fig. 3. The EC_{50} values for the forskolin-induced change in I_{sc} and G_T of tissues bathed in symmetrical NaCl/HCO_3^- Ringer solution are 9.5±1.26 and 0.86±0.24 μmol l^{-1}, respectively. The EC_{50} values for the inhibition of I_{Cl} generated by exposing the tissue to a mucosal to serosal Cl^- gradient is 0.75±0.01 μmol l^{-1}.

In an attempt to determine whether the I_{Cl} seen in the presence of a Cl^- gradient was due to cellular or paracellular Cl^- flow, we investigated the effects of inhibitors of Cl^- transporters that would be involved in transcellular transpoprt of Cl^-. Mucosal GlyH101 (50 μmol l^{-1}) resulted in a rapid inhibition of the I_{Cl} and overall mucosal GlyH101 inhibited 82±4% (N=6) of the forskolin-sensitive I_{Cl}, whereas serosal addition had no effect (Fig. 11A,C). In contrast, mucosal DIDS (1 mmol l^{-1}) had little effect on I_{Cl}, but serosal DIDS profoundly (89±4%, N=6) inhibited the I_{Cl} (Fig. 11B,C). While DIDS inhibits a number of anion channels (Hartzell et al., 2009), it also inhibits a range of transport proteins, some of which are electrogenic (Romero et al., 2004). However, it is unlikely that the inhibitory actions of DIDS resulted from the inhibition of an electrogenic transporter, rather than an anion channel, because NPPB, which inhibits a range of anion channels including pCFTR (Demmers et al., 2010), also inhibited the I_{Cl}, and was as effective from both the mucosal and serosal side (Fig. 11C).

The total I_{Cl} seen in the presence of Cl^- gradients was clearly rectified. In the presence of a serosal to mucosal Cl^- gradient (ΔCl_{sm}) the steady-state I_{Cl} was considerably smaller, and initially it appeared that forskolin did not inhibit the I_{Cl} (Fig. 9). However, immediately following the addition of forskolin there was a transient reduction of the I_{Cl} (Fig. 9A), followed by recovery towards pre-forskolin levels. This reflects an initial inhibition of the gradient-driven I_{Cl} followed by a slower appearance of the forskolin-stimulated anion secretion. Supporting this conclusion is the observation that, following treatment with forskolin, an appreciable GlyH101 sensitive current was apparent in the presence of a ΔCl_{sm}, but not in the presence of a ΔCl_{ms} (Fig. 9B,C). Under the latter conditions the secretory current was inhibited by the removal of Cl^- from the serosal bathing solution. The currents remaining after treatment of tissue bathed in solution with either a ΔCl_{ms} (–25±7.5 μA cm^{-2}) or ΔCl_{sm} (33±4 μA cm^{-2}) with forskolin and GlyH101 were comparable, and presumably reflect the current flow through the paracellular pathway due to the equal but opposite Cl^- gradients. Therefore, assuming that forskolin and GlyH101 have a minimal effect on the paracellular pathway, in the presence of a ΔCl_{sm} a cellular I_{Cl} of ~35 μA cm^{-2} is present, ~10–15% of that seen in the presence of an equivalent mucosal to serosal gradient (~274 μA cm^{-2}).

DISCUSSION

Electrogenic anion secretion dependent upon CFTR appears to be of less significance in the intestine of the possum, a metatherian mammal, than in the intestine of eutherian mammals. For example, in the eutherian small intestine there is an oral–aboral gradient of CFTR expression, with the highest levels of expression in the duodenum and decreasing amounts in the jejunum and ileum (Ameen et al., 2000a; Strong et al., 1994; Trezise and Buchwald, 1991). Associated with this are high levels of electrogenic Cl^- secretion, thought to be essential to the overall function of the small intestine (Field, 2003). In contrast, in the possum, the ileum is the only region of the small intestine that exhibits appreciable expression of CFTR (Gill et al., 2011), and the response of the ileum to cAMP-dependent secretagogues involves HCO_3^- secretion not Cl^- secretion (Gill et al., 2011). Here, we present evidence of a novel pattern of CFTR expression in the possum proximal colon, where CFTR is

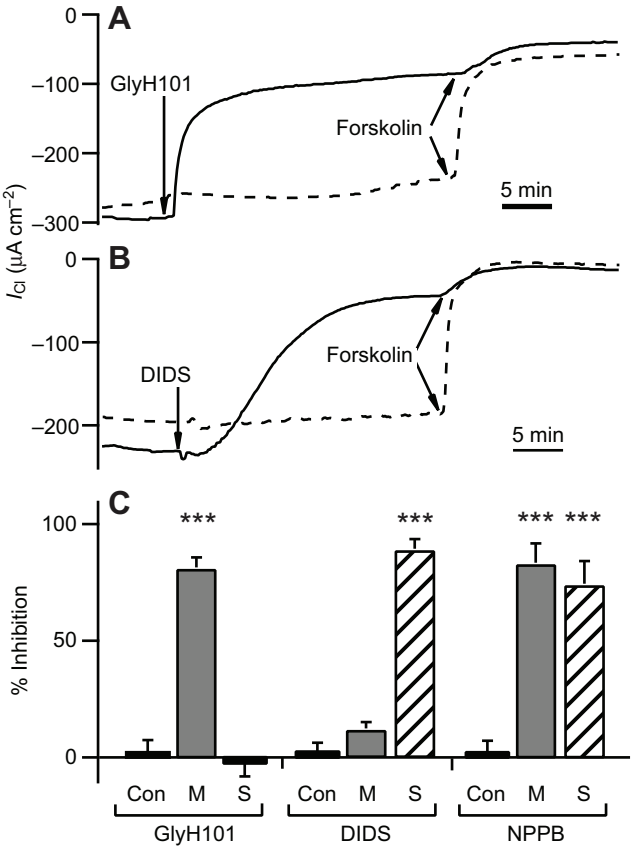

Fig. 11. The effect of GlyH101, DIDS and NPPB on the forskolin-sensitive I_{Cl} measured across the possum colon in the presence of a mucosal to serosal Cl^- gradient. (A) Representative experiment showing that mucosal addition of GlyH101 (50 μmol l^{-1}) resulted in a rapid inhibition of the I_{Cl}. (B) Representative experiment demonstrating the effect of serosal DIDS (1 mmol l^{-1}) on the I_{Cl}. (C) The effect of mucosal (M) or serosal (S) addition of GlyH101 (50 μmol l^{-1}), DIDS (1 mmol l^{-1}) or NPPB (100 μmol l^{-1}) on the I_{Cl}. Vehicle was added to the control tissues. $N \geq 8$. Asterisks indicate significant difference (***$P<0.001$) from respective control, ANOVA with Dunnett's *post hoc* test.

restricted to a small population of CHE cells. This markedly modifies cAMP-stimulated anion secretion in the possum proximal colon when compared with the eutherian proximal colon. More significantly, however, these CHE cells also provide a constitutively active transepithelial Cl^- conductance that is most likely associated with NaCl absorption.

In the eutherian colon, CFTR is expressed primarily in the apical membrane of cells in the basal regions of the crypts, with decreasing levels of expression in the upper crypts and little or no expression in the surface cells (Jakab et al., 2011). The distribution of NKCC1 in the colonic epithelium is similar to that of CFTR, although it is localized to the basolateral membrane, whereas pNBCe1, which is also expressed in the basolateral membrane, is found only in the upper half of the crypts and the surface cells (Jakab et al., 2011). Consequently, in the colon of eutherian mammals secretagogues primarily stimulate electrogenic Cl^- secretion, with a limited amount of electrogenic HCO_3^- secretion (Kunzelmann and Mall, 2002). The pattern of expression of NKCC1 and pNBCe1 in the possum is similar to that of eutherian mammals but, in contrast to the case in the eutherian colon, CFTR in the possum proximal colon is restricted to a small population of CHE cells located in the upper regions of the crypts and the surface cells. This novel distribution of CFTR in the colonic epithelium is supported by the distribution of CFTR mRNA, which shows a punctate distribution, with high levels of CFTR transcript in a limited number of cells in the upper regions of the colonic crypts as well as surface epithelium. Although these CHE cells express high levels of CFTR, they do not appear to express either NKCC1 or pNBCe1, the basolateral transporters normally associated with electrogenic anion secretion in the intestine, as the CFTR-mediated secretory response is not dependent on either pNBCe1 or NKCC1.

Immunolocalization of CFTR is difficult and often it is not possible to demonstrate the expression of CFTR within a cell, despite functional evidence that it is present (Regnier et al., 2008). However, in the possum colon the restriction of CFTR to the CHE cells is supported by the available functional data. Forskolin, which activates pCFTR (Demmers et al., 2010), stimulated an increase in I_{sc} by the possum proximal colon. This was completely inhibited by either mucosal GlyH101 or mucosal NPPB, both of which inhibit pCFTR (Gill et al., 2011), but not DIDS, which inhibits Ca^{2+}-activated Cl^- channels (Yang et al., 2008), indicating that the I_{sc} response to forskolin is dependent upon pCFTR. Given the distribution of NKCC1 and pNBCe1 in the proximal colonic epithelium of the possum, if pCFTR were expressed in cells other than the CHE cells then it would be reasonable to conclude that the forskolin-stimulated I_{sc} would involve either electrogenic Cl^- secretion dependent upon NKCC1 or electrogenic HCO_3^- secretion dependent upon pNBCe1. However, the forskolin-stimulated I_{sc} was not inhibited by bumetanide or DIDS, which inhibit NKCC1 (Gamba, 2005) and pNBCe1 (Romero et al., 2004), respectively. The lack of an effect of DIDS or bumetanide is unlikely to result from an insensitivity of possum pNBCe1 and NKCC1 to these compounds, as DIDS is an effective inhibitor of pNBCe1-dependent HCO_3^- secretion in the possum ileum (Bartolo et al., 2009b) and bumetanide inhibits K^+ secretion in the proximal colon (S.F. and A.G.B., unpublished results). Furthermore, NKCC1 is found in a range of phyla (e.g. elasmobranchs, birds and mammals) and is inhibited by bumetanide in all species tested (Lowy et al., 1989; Palfrey et al., 1984; Russell, 2000).

Given the restriction of pCFTR to the CHE cells and the resultant separation of CFTR from NKCC1 and pNBCe1, what is the function of these cells? CHE cells are also present in the eutherian intestine although, unlike the possum, they are located in the duodenal and jejunal villi (Ameen et al., 1995; Ameen et al., 1999), not the colon. In eutherian mammals, CHE cells are thought to be secretory (Ameen et al., 2000b) and it would appear that the CHE cells of the possum proximal colon may also have a secretory role, although once again the secretory mechanism does not resemble that normally seen in eutherian mammals. Forskolin stimulates an increase in I_{sc}, which is inhibited by CFTR blockers and is dependent upon serosal Na^+, Cl^- and HCO_3^-, all of which is consistent with CFTR-dependent anion secretion. However, although CFTR appears to be involved in this response, the identity of the basolateral transport proteins involved remains uncertain. The CHE cells do not appear to express NKCC1 or pNBCe1 and the pharmacology and ion dependence of the secretory response confirm that it does not involve either NKCC1 or pNBCe1. Furthermore, the absence of an effect of either acetazolamide or EIPA demonstrates that the generation of HCO_3^- for secretion through the hydration of CO_2 by carbonic anhydrase is also not involved. The ion dependence of the secretory response suggests it may involve the possum orthologue of the Na^+-dependent Cl^-/HCO_3^- exchanger (Fig. 12). However, until more is known about the pharmacological profile and distribution

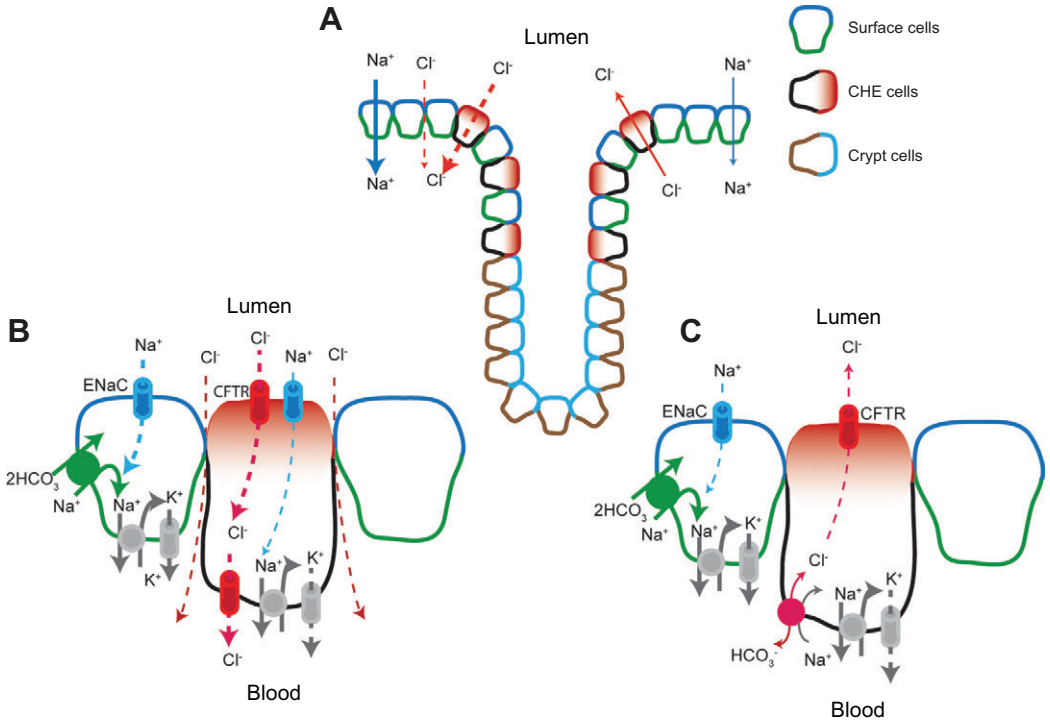

Fig. 12. A summary of the role of CFTR in the possum proximal colon in the presence of high luminal Cl^-. (A) Schematic arrangement of the CHE cells within the crypt–surface cell axis. The left-hand side shows the net transport of ions under basal or spontaneous conditions and the right-hand side shows the net transport of ions in the presence of forskolin. Solid lines indicate active transport processes and dashed lines passive transport. The thickness of the line gives an indication of the relative magnitude of ion transport by a given pathway. (B) The cellular mechanism of transepithelial transport of Na^+ and Cl^- under basal non-stimulated conditions. In the CHE cells, CFTR in series with a basolateral DIDS-sensitive Cl^- conductance provides a transepithelial route for the passive absorption of Cl^- driven by active transport of Na^+ in the surrounding cells. (C) The effect of stimulation with forskolin on the cellular mechanism of transepithelial transport of Na^+ and Cl^-. Forskolin inhibits the passive absorption of Cl^- through inhibition of the basolateral DIDS-sensitive Cl^- conductance. Inhibition of its counter-ion Cl^- limits Na^+ absorption. In addition, forskolin stimulates a basolateral Na^+-dependent anion transporter, potentially a Na^+-dependent Cl^-/HCO_3^- exchanger, which drives CFTR-dependent anion secretion.

of this and other Cl^-- and HCO_3^--dependent transporters in the possum, it is not possible to state which transporter is driving secretion in the CHE cells of the possum proximal colon.

In addition to this secretory role, the CHE cells also appear to have an absorptive role. Mucosal NPPB and GlyH101 decreased the spontaneous G_T of the possum proximal colon, as did serosal DIDS, indicating that CFTR in the apical membrane and a DIDS-sensitive conductance in the basolateral membrane are constitutively active in the proximal colon, and provide a cellular transepithelial anion conductance. Because CFTR is restricted to the CHE cells in the proximal colon, this conductance is presumably a property of the CHE cells and not a general property of all of the colonic epithelial cells (Fig. 12).

In tight Na^+-absorbing epithelia, active electrogenic Na^+ absorption establishes a transepithelial potential that provides the driving force for passive Cl^- absorption. There are several examples of tight Na^+-absorbing epithelia where the counter-ion Cl^- is absorbed *via* a transepithelial cellular Cl^- conductance rather than the paracellular pathway. In the presence of high luminal Cl^- the mitochondria-rich (MR) cells in the amphibian skin provide a high conductance Cl^- pathway (Larsen, 1991; Larsen et al., 2001). In contrast, in the duct of the sweat gland (Quinton, 1983; Quinton, 1986; Reddy and Quinton, 1989b) and maxillary salivary glands (Dinudom et al., 1995) of eutherian mammals, the cellular Cl^- conductance is not restricted to a specific cell type but is a feature of all the epithelial cells. Unlike the CHE cells of the possum, where CFTR is restricted to the apical membrane, in the sweat duct this transepithelial Cl^- conductance involves the expression of CFTR in both the apical and basolateral membrane (Reddy and Quinton, 1992), and in the disease cystic fibrosis the absence of this conductance limits the absorption of fluid and electrolytes from sweat (Quinton, 1986). A characteristic feature of the transport properties of the possum proximal colon is the high level of electrogenic Na^+ absorption (Butt et al., 2002a) and while the proximal colon has a high G_T compared with typical tight Na^+-absorbing epithelia, much of the conductance is a consequence of the transepithelial Cl^- conductance provided by the CHE cells. Therefore, it is likely that the CHE cells in the possum proximal colon provide a high conductance pathway for the absorption of Cl^-, which consists of a series arrangement of CFTR in the apical membrane and a DIDS-sensitive anion conductance in the basolateral membrane. This proposal is supported by the observation that in the presence of a transepithelial Cl^- gradient a I_{Cl} is present that is due primarily to Cl^- flow through the CHE cells, as it is inhibited by mucosal GlyH101 and serosal DIDS.

For the passive movement of Cl^- *via* a cellular transepithelial conductance, appropriate electrochemical gradients are required at the apical and basolateral membrane of the cell. In the sweat duct the apical membrane potential (Ψ_a) is dominated by the Cl^- conductance provided by CFTR (Reddy and Quinton, 1989a). However, Ψ_a is not equivalent to the equilibrium potential for Cl^- (E_{Cl}), because the apical membrane also has an appreciable Na^+ conductance due to ENaC. Hence, Ψ_a is depolarized with respect

to E_{Cl} and as a result there is a driving force for Cl^- entry into the cell across the apical membrane. A similar arrangement exists in the basolateral membrane, but here the Cl^- conductance is in parallel with a K^+ conductance. Consequently, the basolateral membrane potential is hyperpolarized with respect to E_{Cl} and hence there is a driving force for Cl^- exit across the basolateral membrane (Reddy and Quinton, 1987; Reddy and Quinton, 1989a). Passive Cl^- absorption *via* the MR cells in amphibian skin is thought to occur by a similar mechanism (Larsen, 1991) and it is likely that a similar arrangement provides the driving force for Cl^- absorption *via* the CHE cells of the possum proximal colon. If this is the case, it has some consequences, particularly if the luminal Cl^- concentration ($[Cl^-]_L$) is low, which occurs in the colon as short-chain fatty acids are the main luminal anion (Argenzio, 1991). For passive Cl^- absorption to occur in the presence of low $[Cl^-]_L$, Ψ_a must depolarize markedly or cellular Cl^- concentration ($[Cl^-]_i$) fall appreciably to maintain the driving force for Cl^- entry into the cells across the apical membrane. In the sweat duct, while Ψ_a depolarizes and $[Cl^-]_i$ falls in the presence of reduced $[Cl^-]_L$, the changes are not sufficient to maintain the driving force for Cl^- influx (Reddy and Quinton, 1989a). Consequently, under these conditions alternative active mechanisms, such as Cl^-/HCO_3^- exchange, are involved in Cl^- absorption (Reddy and Quinton, 1994). Similarly, in the MRC of the amphibian skin, when $[Cl^-]_L$ is low, Cl^- absorption also involves a Cl^-/HCO_3^- exchanger (Larsen, 1991). Furthermore, the apical Cl^- channels in the MRC are regulated by external Cl^- and voltage in such a way that they are only open when electrochemical gradient for Cl^- favours Cl^- absorption (Willumsen et al., 2002), which serves to limit passive Cl^- loss. When the possum proximal colon was bathed in equal but opposite transepithelial Cl^- gradients the I_{Cl} was clearly rectified, with an ~10-fold greater I_{Cl} in the presence of a mucosal to serosal gradient (i.e. high $[Cl^-]_L$) compared with serosal to mucosal gradient (low $[Cl^-]_L$). This suggests that $[Cl^-]_L$ regulates the transepithelial conductance of the CHE cells. Whether this involves modulation of the apical or basolateral Cl^- conductance in unknown, but it also indicates that in the presence of low $[Cl^-]_L$ in the proximal colon, passive loss of Cl^- *via* this pathway will be limited and alternative active transport mechanisms will be required for Cl^- absorption.

The stimulation of anion secretion by the possum proximal colon required high concentrations of forskolin ($EC_{50} \approx 10\,\mu mol\,l^{-1}$), which explains the lack of response to membrane-permeable analogues of cAMP and cGMP reported previously (Butt et al., 2002a). However, in addition to anion secretion, forskolin also stimulated a decrease in G_T. This occurred at a lower concentration of forskolin ($EC_{50} \approx 1\,\mu mol\,l^{-1}$) compared with the secretory response and may be the primary cAMP-dependent response of the possum proximal colon.

In the eutherian intestine, cAMP modulates the permeability of the paracellular pathway and stimulation of anion secretion is associated with an decrease in G_T due to a modification of the tight junction (Shen et al., 2011). While this may also occur in the possum, it is not the entire explanation for the changes in G_T seen in the proximal colon. Although GlyH101, NPPB and DIDS decreased the spontaneous G_T of the proximal colon, this effect was eliminated following stimulation with forskolin, which also decreased G_T. This suggests that forskolin inhibits the transepithelial Cl^- conductance associated with the CHE cells. Supporting this proposal is the observation that the I_{Cl} that develops in the presence of a Cl^- gradient, and is a consequence of Cl^- flow through the CHE cells, is inhibited by forskolin. However, CFTR is essential for the secretory response stimulated by forskolin. Therefore, it is unlikely that the decrease in G_T induced by forskolin is due to inhibition of CFTR. Rather, it most probably reflects the inhibition of the basolateral DIDS-sensitive conductance (Fig. 12).

This inhibition of the basolateral Cl^- conductance has a number of potentially physiologically relevant roles. Firstly, similar to the manner in which cystic fibrosis limits Na^+ absorption in the sweat duct (Quinton, 1986), the inhibition of the basolateral Cl^- conductance in the proximal colon by forskolin will limit the absorption of Na^+ by restricting the movement of the counter-ion Cl^-. Furthermore, because the basolateral conductance is in the same cells as CFTR, it is possible that the inhibition by forskolin will increase the efflux of anions across the apical membrane and thus increase the secretory response, as has been shown for pulmonary epithelia from *Xenopus laevis* (Berger et al., 2010). The concomitant stimulation of secretion and inhibition of absorption is a common theme in the eutherian intestine (Field, 2003; Kunzelmann and Mall, 2002), and effectively maximizes the shift of the intestine from an absorptive to a secretory state.

In summary, in the possum proximal colon CFTR is restricted to the apical membrane of a small population of CHE cells located in the surface epithelium and upper crypts. In these cells, CFTR is constitutively active and in the presence of a high luminal Cl^- concentration the series arrangement of CFTR with a DIDS-sensitive anion conductance in the basolateral membrane of the CHE cells provides a transepithelial anion conductance. This presumably serves as a conductive pathway for the absorption of Cl^-, and possibly other counter-ions for Na^+, which is absorbed by electrogenic Na^+ transport. Forskolin inhibits the conductance associated with the CHE cells through blockage of the basolateral DIDS-sensitive conductance and this most probably inhibits Na^+ absorption through restriction of the movement of Cl^-. In addition, at higher concentrations forskolin stimulates CFTR-dependent electrogenic anion secretion. However, this is mechanistically different to that seen in the eutherian intestine and possum ileum, and appears to involve a Na^+-dependent Cl^-/HCO_3^- exchanger in the basolateral membrane.

ACKNOWLEDGEMENTS

We thank Euan Thompson for the collection and maintenance of the possums and Bernie McLeod for helpful discussions.

FUNDING

This work was supported by a University of Otago Research Grant and grants from the Foundation for Research Science and Technology, the Animal Health Board NZ Inc., and the National Research Centre for Possum Biocontrol.

REFERENCES

Ameen, N. A., Ardito, T., Kashgarian, M. and Marino, C. R. (1995). A unique subset of rat and human intestinal villus cells express the cystic fibrosis transmembrane conductance regulator. *Gastroenterology* **108**, 1016-1023.

Ameen, N. A., Martensson, B., Bourguinon, L., Marino, C., Isenberg, J. and McLaughlin, G. E. (1999). CFTR channel insertion to the apical surface in rat duodenal villus epithelial cells is upregulated by VIP *in vivo*. *J. Cell Sci.* **112**, 887-894.

Ameen, N., Alexis, J. and Salas, P. (2000a). Cellular localization of the cystic fibrosis transmembrane conductance regulator in mouse intestinal tract. *Histochem. Cell Biol.* **114**, 69-75.

Ameen, N. A., vanDonselaar, E., Posthuma, G., deJonge, H., McLaughlin, G., Geuze, H. J., Marino, C. and Peters, P. J. (2000b). Subcellular distribution of CFTR in rat intestine supports a physiologic role for CFTR regulation by vesicle traffic. *Histochem. Cell Biol.* **114**, 219-228.

Argenzio, R. A. (1991). Comparative physiology of colonic electrolyte transport. In *Handbook of Physiology. The Gastrointestinal System*, vol. IV (ed. S. G. Scultz), pp. 275-285. Bethesda: American Physiological Society.

Bachmann, O., Riederer, B., Rossmann, H., Groos, S., Schultheis, P. J., Shull, G. E., Gregor, M., Manns, M. P. and Seidler, U. (2004). The Na^+/H^+ exchanger isoform 2 is the predominant NHE isoform in murine colonic crypts and its lack causes NHE3 upregulation. *Am. J. Physiol. Gastrointest. Liver Physiol.* **287**, G125-G133.

Bachmann, O., Juric, M., Seidler, U., Manns, M. P. and Yu, H. (2010). Basolateral ion transporters involved in colonic epithelial electrolyte absorption, anion secretion, and cellular homeostasis. *Acta Physiol.* **201**, 33-46.

Bartolo, R., Harfoot, N., Gill, M., Demmers, K., McLeod, B. and Butt, A. G. (2009a). Electrogenic Cl^- secretion does not occur in the ileum of the possum *Trichosurus vulpecula* due to low levels of NKCC1 expression. *J. Comp. Physiol.* **179**, 997-1010.

Bartolo, R., Harfoot, N., Gill, M., McLeod, B. and Butt, A. G. (2009b). Secretagogues stimulate electrogenic HCO_3^- secretion in the ileum of the brushtail possum, *Trichosurus vulpecula*. Evidence for the role of a $NaHCO_3$ cotransporter. *J. Exp. Biol.* **212**, 2645-2655.

Berger, J., Richter, K., Clauss, W. G. and Fronius, M. (2010). Evidence for basolateral Cl^- channels as modulators of apical Cl^- secretion in pulmonary epithelia of *Xenopus laevis*. *Am. J. Physiol. Regul. Integr. Comp. Physiol.* **299**, R92-R100.

Butt, A. G., Mathieson, S. E. and McLeod, B. J. (2002a). Electrogenic ion transport in the intestine of the Australian common brushtail possum, *Trichosurus vulpecula*: indications of novel transport patterns in a marsupial. *J. Comp. Physiol.* **172**, 495-502.

Butt, A. G., Mathieson, S. E. and McLeod, B. J. (2002b). Aldosterone does not regulate amiloride-sensitive Na^+ transport in the colon of the Australian common brushtail possum, *Trichosurus vulpecula*. *J. Comp. Physiol.* **172**, 519-527.

Cuthbert, A. W., Hickman, M. E. and MacVinish, L. J. (1999). Formal analysis of electrogenic sodium, potassium, chloride and bicarbonate transport in mouse colon epithelium. *Br. J. Pharmacol.* **126**, 358-364.

Demmers, K. J., Carter, D., Fan, S., Mao, P., Maqbool, N. J., McLeod, B. J., Bartolo, R. and Butt, A. G. (2010). Molecular and functional characterization of the cystic fibrosis transmembrane conductance regulator from the Australian common brushtail possum, *Trichosurus vulpecula*. *J. Comp. Physiol.* **180**, 545-561.

Dinudom, A., Komwatana, P., Young, J. A. and Cook, D. I. (1995). A forskolin-activated Cl^- current in mouse mandibular duct cells. *Am. J. Physiol. Gastrointest. Liver Physiol.* **31**, G806-G812.

Field, M. (2003). Intestinal ion transport and the pathophysiology of diarrhea. *J. Clin. Invest.* **111**, 931-943.

Gamba, G. (2005). Molecular physiology and pathophysiology of electroneutral cation-chloride cotransporters. *Physiol. Rev.* **85**, 423-493.

Gawenis, L. R., Bradford, E. M., Alper, S. L., Prasad, V. and Shull, G. E. (2010). AE2 Cl^-/HCO_3^- exchanger is required for normal cAMP-stimulated anion secretion in murine proximal colon. *Am. J. Physiol. Gastrointest. Liver Physiol.* **298**, G493-G503.

Gill, M., Bartolo, R. C., Demmers, K., Fan, S., Harfoot, N. and Butt, A. G. (2011). The distribution and expression of CFTR restricts electrogenic anion secretion to the ileum of the brushtail possum, *Trichosurus vulpecula*. *J. Exp. Biol.* **214**, 1943-1954.

Grubb, B. R. (1997). Ion transport across the murine intestine in the absence and presence of CFTR. *Comp. Biochem. Physiol.* **118A**, 277-282.

Hartzell, H. C., Yu, K., Xiao, Q., Chien, L. T. and Qu, Z. (2009). Anoctamin/TMEM16 family members are Ca^{2+}-activated Cl^- channels. *J. Physiol.* **587**, 2127-2139.

Jakab, R. L., Collaco, A. M. and Ameen, N. A. (2011). Physiological relevance of cell-specific distribution patterns of CFTR, NKCC1, NBCe1, and NHE3 along the crypt-villus axis in the intestine. *Am. J. Physiol. Gastrointest. Liver Physiol.* **300**, G82-G98.

Karasov, W. H. and Hume, I. D. (1997). Veterbrate gastrointestinal system. In *Handbook of Physiology*, Section 13, *Comparative Physiology*, vol. 1 (ed. W. H. Dantzler), pp. 409-480. New York: Oxford University Press.

Knutson, T. W., Koss, M. A., Hogan, D. L., Isenberg, J. I. and Knutson, L. (1995). Acetazolamide inhibits basal and stimulated HCO_3^- secretion in the human proximal duodenum. *Gastroenterology* **108**, 102-107.

Kunzelmann, K. and Mall, M. (2002). Electrolyte transport in the mammalian colon: mechanisms and implications for disease. *Physiol. Rev.* **82**, 245-289.

Larsen, E. H. (1991). Chloride transport by high-resistance heterocellular epithelia. *Physiol. Rev.* **71**, 235-283.

Larsen, E. H., Kristensen, P., Nedergaard, S. and Willumsen, N. J. (2001). Role of mitochondria-rich cells for passive chloride transport, with a discussion of Ussing's contribution to our understanding of shunt pathways in epithelia. *J. Membr. Biol.* **184**, 247-254.

Leppilampi, M., Parkkila, S., Karttunen, T., Gut, M. O., Gros, G. and Sjoblom, M. (2005). Carbonic anhydrase isozyme-II-deficient mice lack the duodenal bicarbonate secretory response to prostaglandin E_2. *Proc. Natl. Acad. Sci. USA* **102**, 15247-15252.

Lowy, R. J., Dawson, D. C. and Ernst, S. A. (1989). Mechanism of ion transport by avian salt gland primary cell cultures. *Am. J. Physiol. Regul. Integr. Comp. Physiol.* **256**, R1184-R1191.

Palfrey, H. C., Silva, P. and Epstein, F. H. (1984). Sensitivity of cAMP-stimulated salt secretion in shark rectal gland to 'loop' diuretics. *Am. J. Physiol. Cell Physiol.* **246**, C242-C246.

Quinton, P. (1983). Chloride permeability in cystic fibrosis. *Nature* **301**, 421-422.

Quinton, P. M. (1986). Missing Cl conductance in cystic fibrosis. *Am. J. Physiol. Cell Physiol.* **251**, C649-C652.

Reddy, M. M. and Quinton, P. M. (1987). Intracellular potentials of microperfused human sweat duct cells. *Pflügers Arch.* **410**, 471-475.

Reddy, M. M. and Quinton, P. M. (1989a). Altered electrical potential profile of human reabsorptive sweat duct cells in cystic fibrosis. *Am. J. Physiol. Cell Physiol.* **257**, C722-C726.

Reddy, M. M. and Quinton, P. M. (1989b). Localization of Cl^- conductance in normal and Cl^- impermeability in cystic fibrosis sweat duct epithelium. *Am. J. Physiol. Cell Physiol.* **257**, C727-C735.

Reddy, M. M. and Quinton, P. M. (1992). cAMP activation of CF-affected Cl^- conductance in both cell membranes of an absorptive epithelium. *J. Membr. Biol.* **130**, 49-62.

Reddy, M. M. and Quinton, P. M. (1994). Intracellular Cl activity: evidence of dual mechanisms of cl absorption in sweat duct. *Am. J. Physiol. Cell Physiol.* **267**, C1136-C1144.

Regnier, A., Dannhoffer, L., Biouquit-Laye, S., Bakari, M., Naline, E. and Chinet, T. (2008). Expression of cystic fibrosis transmembrane conductance regulator in the human distal lung. *Hum. Pathol.* **39**, 368-376.

Romero, M. F., Fulton, C. M. and Boron, W. F. (2004). The SLC4 family of HCO_3^- transporters. *Pflugers Arch.* **447**, 495-509.

Russell, J. M. (2000). Sodium-potassium-chloride cotransport. *Physiol. Rev.* **80**, 211-276.

Schmitt, B. M., Biemesderfer, D., Romero, M. F., Boulpaep, E. L. and Boron, W. F. (1999). Immunolocalization of the electrogenic Na^+-HCO_3^- cotransporter in mammalian and amphibian kidney. *Am. J. Physiol. Renal Physiol.* **276**, F27-F38.

Schultheis, P. J., Clarke, L. L., Meneton, P., Miller, M. L., Soleimani, M., Gawenis, L. R., Riddle, T. M., Duffy, J. J., Doetschman, T., Wang, T. et al. (1998). Renal and intestinal absorptive defects in mice lacking the NHE3 Na^+/H^+ exchanger. *Nat. Genet.* **19**, 282-285.

Seamon, K. B., Padgett, W. and Daly, J. W. (1981). Forskolin: unique diterpene activator of adenylate cyclase in membranes and in intact cells. *Proc. Natl. Acad. Sci. USA* **78**, 3363-3367.

Shen, L., Weber, C. R., Raleigh, D. R., Yu, D. and Turner, J. R. (2011). Tight junction pore and leak pathways: a dynamic duo. *Annu. Rev. Physiol.* **73**, 283-309.

Strong, T. V., Boehm, K. and Collins, F. S. (1994). Localization of cystic fibrosis transmembrane conductance regulator mRNA in the human gastrointestinal tract by *in situ* hybridization. *J. Clin. Invest.* **93**, 347-354.

Trezise, A. E. and Buchwald, M. (1991). *In vivo* cell-specific expression of the cystic fibrosis transmembrane conductance regulator. *Nature* **353**, 434-437.

Willumsen, N. J., Amstrup, J., Møbjerg, N., Jespersen, A., Kristensen, P. and Larsen, E. H. (2002). Mitochondria-rich cells as experimental model in studies of epithelial chloride channels. *Biochim. Biophys. Acta* **1566**, 28-43.

Yang, Y. D., Cho, H., Koo, J. Y., Tak, M. H., Cho, Y., Shim, W. S., Park, S. P., Lee, J., Lee, B., Kim, B. M. et al. (2008). TMEM16A confers receptor-activated calcium-dependent chloride conductance. *Nature* **455**, 1210-1215.